Distinctly Different Interactions of Anesthetic and Nonimmobilizer with Transmembrane Channel Peptides

Pei Tang, Jian Hu, Serguei Liachenko, and Yan Xu
Department of Anesthesiology and Critical Care Medicine, Department of Pharmacology, University of Pittsburgh, Pittsburgh, Pennsylvania 15261 USA

ABSTRACT Although it plays no clinical role in general anesthesia, gramicidin A, a transmembrane channel peptide, provides an excellent model for studying the specific interaction between volatile anesthetics and membrane proteins at the molecular level. We show here that a pair of structurally similar volatile anesthetic and nonimmobilizer (nonanesthetic), 1-chloro-1,2,2-trifluorocyclobutane (F3) and 1,2-dichlorohexafluorocyclobutane (F6), respectively, interacts differently with the transmembrane peptide. With 400 μM gramicidin A in a vesicle suspension of 60 mM phosphatidylcholine-phosphatidylglycerol (PC/PG), the intermolecular cross-relaxation rate constants between ^{19}F of F3 and ^{1}H in the chemical shift regions for the indole and backbone amide protons were 0.0106 $\pm$ 0.0007 (n = 12) and 0.0105 $\pm$ 0.0014 (n = 8) s^{-1}, respectively. No cross-relaxation was measurable between ^{19}F of F6 and protons in these regions. Sodium transport study showed that with 75 μM gramicidin A in a vesicle suspension of 66 mM PC/PG, F3 increased the ^{23}Na apparent efflux rate constant from 149.7 $\pm$ 7.2 of control (n = 3) to 191.7 $\pm$ 12.2 s^{-1} (n = 3), and the apparent influx rate constant from 182.1 $\pm$ 15.4 to 222.8 $\pm$ 21.7 s^{-1} (n = 3). In contrast, F6 had no effects on either influx or efflux rate. It is concluded that the ability of general anesthetics to interact with amphipathic residues near the peptide-lipid-water interface and the inability of nonimmobilizer to do the same may represent some characteristics of anesthetic-protein interaction that are of importance to general anesthesia.

INTRODUCTION

The century-long quest for the mechanisms of general anesthesia remains a clinical and scientific challenge (Franks and Lieb, 1994). To date, the vast majority of investigations at the molecular level are indirect in nature, inferring mechanisms based on the observed effects of general anesthetics. Not enough attention has been paid to the direct interaction at the molecular level between an anesthetic molecule and a central nervous system site. In particular, when transmembrane proteins are under consideration, little is known about the nature of the sites of such interactions (Eckenhoff and Johansson, 1997).

Sensitivity to general anesthetics has been used as one of the important criteria for identifying proteins that are possibly involved in general anesthesia. A superfamily of ligand-gated ion channels (Franks and Lieb, 1996), which are highly sensitive to general anesthetics, has been the subject of intensive investigations. At the current stage, however, these ligand-gated channels are too complex to allow for structural analysis. A simplified membrane protein model may therefore prove useful in the study of the unifying nature of anesthetic-protein interaction that may be generalized for more complicated systems.

As a simplified model, the well-characterized gramicidin A channel (HCO-L-Val^{1}-Gly^{2}-L-Ala^{3}-D-Leu^{4}-L-Ala^{5}-D-Val^{6}-L-Val^{7}-D-Val^{8}-L-Trp^{9}-D-Leu^{10}-L-Trp^{11}-D-Leu^{12}-L-Trp^{13}-D-Leu^{14}-L-Trp^{15}-NHCH$_2$CH$_2$OH) offers at least the following four advantages, which are unavailable in many other systems: 1) high achievable nuclear magnetic resonance (NMR) spectral resolution of the peptide permits absolute identification of individual amino acid residues along the transmembrane channel (Arseniev et al., 1985; Cross, 1994; Hinton, 1996), thus allowing direct quantitation of the site-specific interaction between anesthetics and the channel peptide; 2) a spectroscopically resolved protein-lipid interface allows testing of popular hypotheses relating to the protein-lipid interaction; 3) an environment that is unique to membrane proteins but not to soluble proteins can be unambiguously defined at the interfacial region, where protein, lipid, and water come into contact; and 4) because gramicidin forms a functional channel with resolved three-dimensional structures, it provides a unique system for determining the structural and functional consequences of anesthetic interaction.

The use of structurally similar pairs of general anesthetics and nonimmobilizers (originally referred to as "nonanesthetics") has attracted much attention in recent years (Koblin et al., 1994; Tang et al., 1997; Ionescu et al., 1994; Raines, 1996; Forman and Raines, 1998; North and Cafiso, 1997). Although each anesthetic or nonimmobilizer cannot verify the relevance of a molecular site to general anesthesia, many nonimmobilizers as a group, in comparison with their anesthetic pairs, may help to identify the characteristics that are shared by all anesthetics but not by the nonimmobilizers (Xu et al., 1998). In protein-free lipid vesicles, we have shown that anesthetics and nonimmobilizers had different submacromolecular distribution in the lipid bilayers (Tang et al., 1997). The anesthetics, such as 1-chloro-

Received for publication 29 January 1999 and in final form 28 April 1999.
Address reprint requests to Dr. Pei Tang, W-1357 Biomedical Science Tower, University of Pittsburgh, Pittsburgh, PA 15261. Tel.: 412-383-9798; Fax: 412-648-9587; E-mail: tang@smtp.anes.upmc.edu.

0006-3495/99/08/739/08 $2.00

1,2,2-trifluorocyclobutane (F3) and isoflurane, preferentially distribute to regions with easy access to the aqueous phase, whereas the structurally similar nonimmobilizers, such as 1,2-dichlorohexafluorocyclobutane (F6) and 2,3-dichlorooctofluorobutane (F8), dwell in the lipid core of the membrane. We have suggested that such a different distribution of anesthetics and nonimmobilizers may ultimately affect their affinity for other membrane constituents, particularly transmembrane proteins.

In the present study, we analyzed the specific interaction of F3 and F6 with gramicidin A, using intermolecular truncated driven nuclear Overhauser effects (TNOEs) (Xu and Tang, 1997). The functional consequences of sodium transport across the gramicidin A channel after interacting with F3 or F6 were also investigated, using the magnetization inversion transfer (MIT) experiments (Hinton et al., 1994).

MATERIALS AND METHODS

Materials

L-α-Phosphatidylcholine (PC) and L-α-phosphatidylglycerol (PG) (egg-sodium salt) were purchased from Avanti Polar Lipids (Alabaster, AL). Gramicidin A was purchased from Calbiochem (La Jolla, CA). Other chemicals, including tripolyphosphate (PPP) and $DyCl_3$ (for preparation of ^{23}Na shift reagent), 2,2,2-trifluoroethanol (TFE), 2,2-dimethyl-2-silapentane-5-sulfonic acid (DSS), NaCl, and Na_2HPO_4 were obtained from Sigma (St. Louis, MO). D_2O was purchased from Cambridge Isotope Laboratories (Andover, MA). F3 and F6 (Fig. 1) were purchased from PCR (Gainesville, FL). All compounds were used without further purification.

Sample preparation

To obtain high-resolution ^1H-NMR spectra of gramicidin A for spectral identification of different residues, gramicidin A was incorporated into sodium dodecyl sulfate (SDS) micelles by the same procedure as described previously (Tang et al., 1999). The procedure ensures the formation of the head-to-head β6.3 dimers that are believed to be identical to the channel structure found in the lipid bilayers. For the TNOE experiments, sonicated vesicles of PC and PG in a 4:1 mole ratio, prepared as described previously (Xu and Tang, 1997), was used. The mean vesicle diameter was 130–160 nm. To incorporate gramicidin A channel into the vesicles, aliquots of 50 mM gramicidin solution in TFE were added, and the vesicle suspension was incubated at 50°C for 3 h. Thereafter, the samples were cooled to room temperature and dialyzed in three exchanges against 4 liters of buffer for 6 h. Complete removal of TFE was confirmed by ^{19}F NMR. The final gramicidin concentration was 400 μM in 60 mM total lipid concentration, with pH adjusted to 6.5. For each NMR experiment, 2 ml of vesicle suspension was placed in a gas-tight, 10-mm-diameter, high-precision NMR tube (Wilmad Glass Co., Buena, NJ), with ~11.5 ml vapor space above the suspension. F3 or F6 was added to a final concentration of 2 mM in the vesicle suspension.

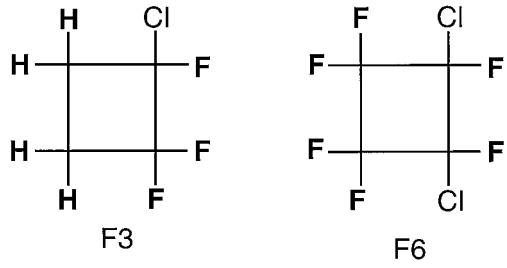

FIGURE 1 Chemical structures of the anesthetic 1-chloro-1,2,2-trifluorocyclobutane (F3) and the structurally similar nonimmobilizer 1,2-dichlorohexafluorocyclobutane (F6).

For MIT measurements, large unilamellar vesicles (LUVs) were prepared to ensure sufficient ^{23}Na signal from inside the vesicles. The extrusion method (Mayer et al., 1986) was employed using a LiposoFast extrusion device (Avestin, Ottawa, Cananda) with polycarbonate filters of defined pore sizes. The size and homogeneity of the LUV population were confirmed by light scattering, using a Coulter N4SD particle size analyzer (Coulter Electronics, Hialeah, FL). For a typical sample, the total lipid concentration was 66 mM. The solutions inside and outside the vesicles contained 100 mM NaCl and were buffered with 10 mM K_2HPO_4/H_3PO_4 to a pH of 8.2.

A special procedure was followed to incorporate gramicidin A into LUV, so that no contamination exists from even a trace amount of organic solvents, which are often general anesthetics. Briefly, PC and PG in a 4:1 molar ratio were first mixed in chloroform and then dried to a thin film under a stream of N_2 gas. Residual chloroform was further removed by high vacuum. After hydration with a buffer with a precalculated Na^+ concentration, aliquots of gramicidin A stock solution (25 mM in TFE) were added to reach the desired gramicidin-to-lipid ratio. The mixture was then incubated at 50°C for 3 h. Thereafter, the mixture was rapidly frozen in CO_2/acetone, lyophilized overnight at −50°C, and vacuumed at room temperature for an additional 24 h. The completely dried samples were then rehydrated without shaking for 2–3 h before the LUV extrusion. The final concentrations of gramicidin A ranged from 0 to 75 μM.

The ^{23}Na chemical shift reagent, $Na_7[DyPPP_2]$, was prepared as previously described (Gupta and Gupta, 1982; Chu et al., 1984) and used for the MIT experiments. The concentration of the shift reagent outside the vesicles was 3.9 mM. For each MIT experiment, 0.6 ml LUV suspension was used in a high-precision 5-mm NMR tube, which had 1.9-ml vapor space above the suspension. F3 and F6 were titrated into the LUV suspension to a total concentration in suspension of 6.9 and 6.3 mM, respectively. Because the ratio of molar solubility of F3 in lipid and in water is ~3000 (Tang et al., 1997), it can be estimated that for 6.9 mM overall concentration of F3 in a 66 mM lipid vesicle suspension, there are 27×10^{-6} moles of F3 per mole of water or, equivalently, 1.5 mM F3 in the aqueous phase. This concentration is clinically relevant (Kendig et al., 1994).

NMR measurements

The MIT and TNOE experiments were conducted at 25°C and 37°C, respectively, using an Otsuka-Chemagnetics (Fort Collins, CO) CMXW-400SLI spectrometer equipped with a four-nucleus probe (J S Research, Boston, MA). The resonance frequencies for ^{23}Na and ^{19}F are 106.1 and 377.4 MHz, respectively. To determine the ^1H resonance frequencies of gramicidin A in PC/PG vesicles, a sample with a 1:33 peptide-to-lipid ratio was prepared and used for magic angle spinning (MAS) ^1H NMR measurements. A selective excitation with a 2.25-ms, 820-mG square pulse was centered at 10 ppm to increase the detection sensitivity of the indole and backbone amide protons and to minimize the water signal (Le Guerneve and Seigneuret, 1996).

The intermolecular ^{19}F-$\{^1H\}$ TNOE was measured between ^{19}F of F3 or F6 and ^1H of gramicidin in selected frequency regions. In the TNOE pulse sequence, $P_{ts}(^1H)$-$P_{90°}(^{19}F)$-$Acq(^{19}F)$-T_R, a selected group of protons was saturated by a highly frequency-selective adiabatic pulse train, $P_{ts}(^1H)$, which consisted of low-power, 90-ms, hyperbolic secant-shaped inversion pulses (Silver et al., 1984; Noggle and Schirmer, 1971) interleaved with 10-ms delays. The total saturation time, t_s, was varied among 11 predetermined values: t_s = 0, 0.5, 1, 2, 3, 4, 5, 6, 8, 10, and 14 s, the order of which was randomized in the experiments. After saturation, a 90° excitation pulse was applied to ^{19}F, followed by ^{19}F data acquisition. The nominal 90° pulse length for ^{19}F was 25 μs. For all ^{19}F spectra, 16 scans were summed in 8192 complex points, with a recycle delay of T_R to ensure full relaxation of the ^{19}F magnetization after each excitation. To minimize any unforeseen

effects of T_1 relaxation, the T_R was varied such that $t_s + T_R$ = constant = 20 s, which was ~6–8 times the T_1 of ^{19}F in the lipid vesicle suspension.

The MIT pulse sequence (Hinton et al., 1994) consisted of three nonselective 90° pulses, $P(90)_x$-t_1-$P(90)_x$-t_2-$P(90)_x$-Acq. In the presence of 3.9 mM $DyPPP_2$ to separate the ^{23}Na signals from the inside and outside of the vesicles ($^{23}Na_{in}$ and $^{23}Na_{out}$, respectively), the transmitter frequency was placed on the resonance of $^{23}Na_{out}$. The nominal 90° pulse was 11 μs. The duration t_1 was precisely set to the reciprocal of twice the chemical shift difference between $^{23}Na_{in}$ and $^{23}Na_{out}$. The mixing time t_2 was incremented from 0.015 to 500 ms; ~30 mixing times were used for each experiment. Typically, the repetition delay between two acquisitions was 400 ms; the spectral width was 4 kHz; and 512 complex points were collected and zero-filled once before Fourier transformation.

Statistical analysis

The method for processing the TNOE data has been elaborated previously (Xu and Tang, 1997). Briefly, for one I spin and N equivalent S spins (e.g., $I = {}^{19}F$ and $S = {}^{1}H$), the NOE, η, measured by the I spin while the S spins are saturated for a period of t_s, is given by

$$\eta_I(t_S) \equiv \frac{I(t_S) - I^0}{I^0} = \frac{\gamma_S}{\gamma_I} \frac{\left\langle \sum_{i=1}^{N} \sigma_{I-Si} \right\rangle}{\rho_{1_I}^*} (1 - e^{-\rho_{1I}^* t_S}) \qquad (1)$$

where $\langle \Sigma \sigma_{Isi}(t) \rangle$ and ρ_1^* ($= 1/T_{1d\text{-}d}$) are the time-averaged intermolecular cross-relaxation rate constant and the direct dipolar relaxation rate constant, respectively; the subscripts denote the associated spins; the superscript 0 indicates the thermal equilibrium state; and γ denotes the gyromagnetic ratio. Thus, by measuring $I(t_s)$ and calculating η_I as a function of S saturation time (t_s), $\langle \Sigma \sigma_{I\text{-}Si} \rangle$ and ρ_{1I}* can be determined by nonlinear regression, using Eq. 1.

For the MIT experiments, one considers the modified Solomon equations for the magnetization inside (I) and outside (S) the vesicles:

$$\frac{dI}{dt} = -\frac{1}{T_1}(I - I_0) - k_e I + k_i S \qquad (2)$$

$$\frac{dS}{dt} = -\frac{1}{T_1'}(S - S_0) - k_i S + k_e I \qquad (3)$$

where T_1 and T_1' are the longitudinal relaxation times of I and S, respectively, and k_i and k_e are the apparent unidirectional influx and efflux rates, respectively. Using the thermal equilibrium relationship $k_e I_0 = k_i S_0$, it is straightforward to solve Eqs. 2 and 3 under the specific initial conditions, which depend on whether I or S is selectively inverted.

If S magnetization is inverted, we have (assuming $T_1 \approx T_1'$, which is true for $^{23}Na_{in}$ and $^{23}Na_{out}$)

$$I = I_0\left[1 - \frac{2k_e}{k_i + k_e} e^{-(t/T_1)}(1 - e^{-(k_i + k_e)t})\right] \qquad (4)$$

$$S = S_o\left[1 - \frac{2}{k_i + k_e} e^{-(t/T_1)}(k_e + k_i e^{-(k_i + k_e)t})\right] \qquad (5)$$

Thus, by measuring I and S as a function of inversion recovery time (with I_0 and S_0 being measured experimentally from the fully relaxed spectra), k_i, k_e, and T_1 can be determined simultaneously by nonlinear regression, using Eqs. 4 and 5.

Parameters from nonlinear regression are expressed as "the best estimates ± standard errors of estimates" (Glantz and Slinker, 1990). To determine the effects of F3 and F6 on a given parameter, the t statistics are calculated as the ratio of the difference between the best estimates of that parameter to the standard error of the difference. A p value of <0.05 is considered statistically significant.

RESULTS

Specific interaction between anesthetic (or nonimmobilizer) molecules and gramicidin A can be quantified by intermolecular truncated driven NOE (Navon et al., 1996; Xu and Tang, 1997). Site selection can be achieved by narrow-band adiabatic saturation of a particular group of protons without affecting others. To demonstrate that such selections are feasible for gramicidin A, high-resolution ^1H spectra of gramicidin A in SDS micelles were used. Fig. 2 shows a stack plot of spectra in the regions of backbone and indole amide protons. The vertical arrows indicate the frequencies of the selective saturation by the hyperbolic secant-shaped pulse train. Clearly, with careful adjustment of pH to avoid base-catalyzed exchange with water (Arseniev et al., 1985; Hinton, 1996), saturation is well localized to the protons selected. Although high ^1H resolution is easily achievable in SDS, intermolecular NOE build-up is more favorable in a lipid bilayer environment. In the channel conformation, gramicidin A forms head-to-head β-6.3 helical dimers (Arseniev et al., 1985). Recent investigations in lipids (Wein-

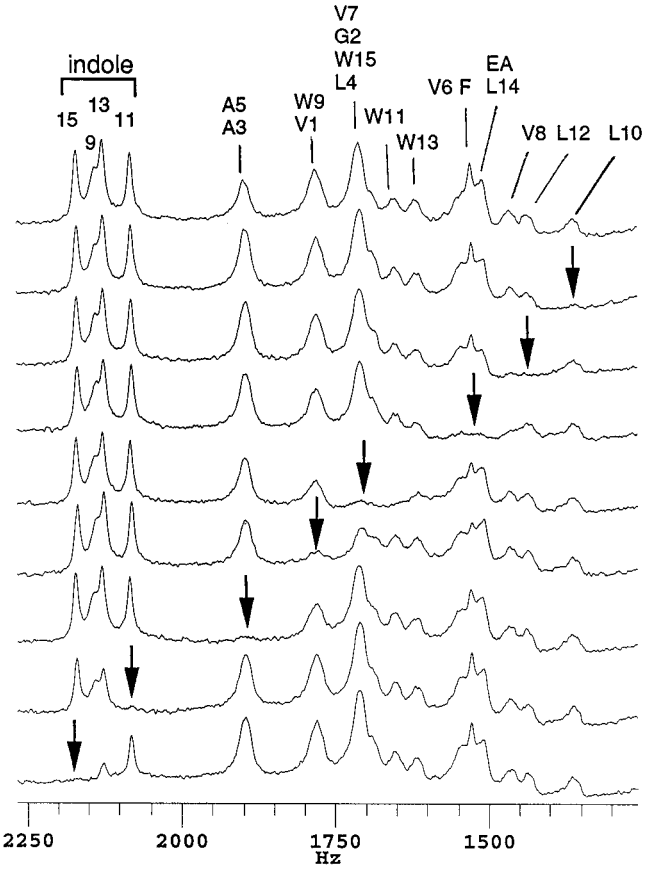

FIGURE 2 High-resolution ^1H spectra of gramicidin A channel in SDS micelles, demonstrating the excellent selective saturation of individual proton groups by the hyperbolic secant-shaped pulse trains. Arrows above each spectrum indicate the frequency at which the selective saturation is centered. To emphasize the narrow selectivity, the frequency axis is plotted in units of Hz relative to the water resonance at 401.102 MHz. Thus the frequency of W15 indole amide proton is at 10.10 ppm, and that of A3 and A5 backbone amide proton is at 9.42 ppm.

stein et al., 1979; Killian et al., 1994; Cross, 1994, 1997; Ketchem et al., 1997; Mobashery et al., 1997) showed that the channel has the same secondary structure in lipid bilayers as in SDS micelles. Given the narrow ^{1}H chemical shift range, it can be assumed that the chemical shifts for most protons in the gramicidin A channel in SDS does not differ greatly from those in lipid vesicles. This is particularly true for the indole N-H protons, as we have observed a distinct indole N-H peak in high-resolution MAS ^{1}H NMR spectra of gramicidin channels in PC/PG lipid bilayers. As reported by others (Le Guerneve and Seigneuret, 1996), the peak is at the same chemical shift range as shown in Fig. 2 for the indole N-H protons and is absent in pure lipid sample without gramicidin. Using the same adiabatic pulse train for site selection in a series of intermolecular ^{19}F-$\{^{1}H\}$ TNOE experiments, we measured selective cross-relaxation rates between ^{19}F of F3 or F6 and ^{1}H of gramicidin A in PC/PG vesicles (Fig. 3). In the absence of gramicidin A, selective saturation at 8.79 and 10.03 ppm, which would correspond to resonance of the backbone and indole N-H protons, respectively, produced no NOE in either F3 or F6. After the addition of 400 μM gramicidin A, the anesthetic F3 gave rise to a $\langle\Sigma\sigma\rangle$ of $0.0105 \pm 0.0014\ s^{-1}$ ($n = 8$) and 0.0106 ± 0.0007 ($n = 12$) with backbone and indole amide protons, respectively. The nonimmobilizer F6, again, showed no measurable cross-relaxation with either the indole or the backbone amide protons. It should be pointed out that although the intermolecular NOE is small, as would be expected, the NOE in F3 is not due to artifacts such as nonspecific saturation through lipids or through intramolecular ^{19}F-$\{^{1}H\}$ NOE. The best proof of this is that the same experiments in the absence of gramicidin showed no observable changes in F3 intensity (*open symbols* in Fig. 3).

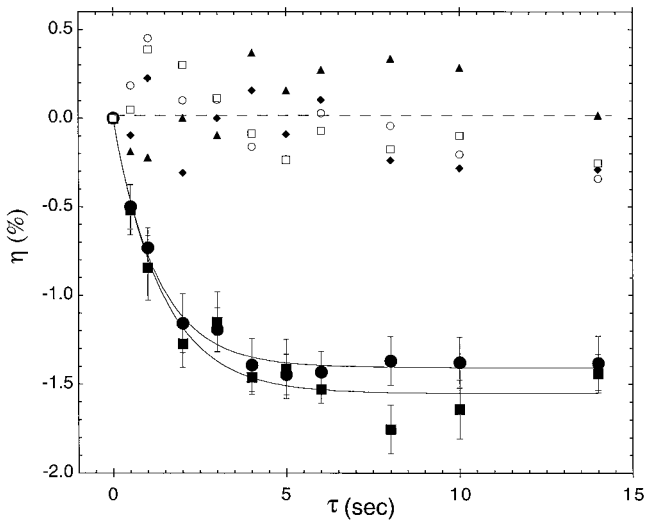

FIGURE 3 Truncated driven ^{19}F-$\{^{1}H\}$ NOE selected in the backbone amide proton region at 8.79 ppm (□, ■, ◆) and the indole N-H proton region at 10.03 ppm (○, ●, ▲) to ^{19}F in F3 (□, ■, ○, ●) or F6 (◆, ▲). Open and filled symbols are measurements in the absence and presence of gramicidin, respectively. With 400 μM gramicidin A, $\langle\Sigma\sigma\rangle$ between F3 and the backbone and indole amide protons was 0.0105 ± 0.0014 ($n = 8$) and 0.0106 ± 0.0007 ($n = 12$), respectively. Solid lines are best fit to the data using Eq. 1. The dashed line is a visual guide indicating no NOE build-up in either F3 in the absence of gramicidin or in F6 in the presence of gramicidin. Error bars show the standard error of the mean.

The distinction between F3 and F6 was also apparent in their ability to affect the function of the gramicidin A channel. Fig. 4 shows two stack plots of ^{23}Na NMR spectra of MIT experiments. In the absence of gramicidin A, the unfacilitated sodium transport was too slow on the NMR time scale to affect the $^{23}Na_{in}$ signal when the outside $^{23}Na_{out}$ was returning to the thermal equilibrium state after its inversion (*right*). In the presence of gramicidin A, however, the intensity profile of the $^{23}Na_{in}$ signal is modulated by the relaxation of $^{23}Na_{out}$ (*left*) due to transport of the inverted magnetization. Representative $^{23}Na_{in}$ signal profiles under the control condition and in the presence of F3 and F6 are plotted in Fig. 5. As shown, F3 at physiological concentrations produced a significant increase ($p < 0.05$) in the unidirectional rates of ^{23}Na transport across the gramicidin A channels, whereas a similar concentration of F6 had little effect on the transport.

DISCUSSION

Prodigious evidence suggests that general anesthetics exert their primary action by interacting with excitable membrane proteins (Franks and Lieb, 1994, 1996; Mihic et al., 1997). The characteristics of such interactions, however, remain unidentified. Despite its structural simplicity and apparent lack of clinical relevance to general anesthesia, gramicidin A channel showed different functional responses to F3 and F6 in our MIT experiments. The parallelism between pharmacological profiles of these agents and their effects on sodium transport suggests that the characteristics of anesthetic-protein interaction found in this simplified system can potentially be generalized. For example, in lipid bilayers, it has been shown (Tang et al., 1997; Xu and Tang, 1997; North and Cafiso, 1997) that the anesthetics are in rapid exchange among all submacromolecular environments, with certain preference for the amphipathic lipid-water interface (Tang et al., 1997; Xu and Tang, 1997; Yoshino et al., 1998). Nonimmobilizers, in contrast, partition deep into the lipid core. This distinction may result from different distributions of partial atomic charges in the anesthetic and nonimmobilizer molecules. The structures in Fig. 1 illustrate a general tendency commonly found in anesthetics and nonimmobilizers, that is, general anesthetics often possess permanent or inducible displacement of partial charges, whereas nonimmobilizers are likely to be apolar (Trudell et al., 1998). Thus the four hydrogen atoms (more electropositive) and four halogen atoms (more electronegative) on two separate sides of F3 molecule make F3 more adaptable to the membrane interface, where a large dipolar potential exists. It has been suggested that modulation of the membrane dipole potential by anesthetics with polarizable or permanent dipole moments may play a significant role in the action of general anesthetics (Cafiso, 1998).

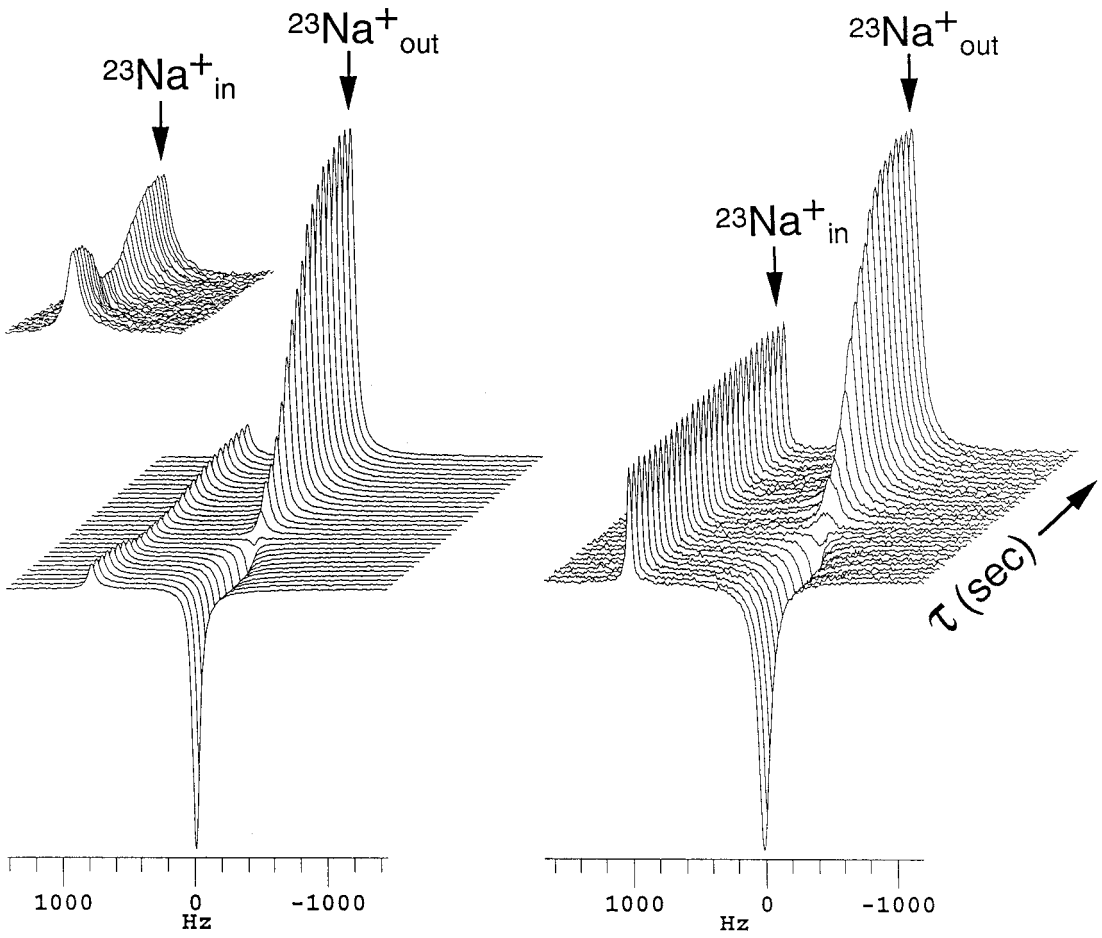

FIGURE 4 Stack plots of $^{23}Na^+$ magnetization inversion transfer (MIT) spectra in the presence (*left*) and absence (*right*) of gramicidin channels. Intra- and extravesicular $^{23}Na^+$ signals are separated by 3.9 mM $DyPPP_2$, a sodium shift reagent. The inset at the upper left corner shows the detailed changes in the intensity profile of $^{23}Na^+_{in}$ due to Na^+ transport.

The difference in submacromolecular distribution of anesthetics and nonimmobilizers is likely to control their ability to interact with the transmembrane channel peptide. As we have shown previously with the channel surface map, there are four amphipathic domains at each end of the gramicidin A channel (Xu et al., 1998). These domains are attributable mainly to four tryptophan residues in each gramicidin molecule. The π-electron distributions in the indole rings may interact with the electropositive moiety of the anesthetic molecules by mechanisms similar to the cation-π type of interaction (Cubero et al., 1998). Indeed, our TNOE results in this study (Fig. 3) show that the anesthetic F3 interacts specifically with the tryptophan side chains, whereas the nonimmobilizer F6 showed no measurable interaction in this region. In separate 2D NOESY experiments with gramicidin A in SDS (Tang et al., 1999), we have found the same tendency under high-resolution conditions. The NOESY spectra revealed that whereas both F3 and F6 caused changes in chemical shift of the backbone N-H resonance of Val^7 deep inside the bilayer, only F3, but not F6, produced significant changes in the interfacial tryptophan indole N-H proton resonance.

Interaction with tryptophan residues in the gramicidin channel may prove to be nontrivial. The critical roles of tryptophan in the gramicidin channel function are at least twofold. First, each of the indole rings is uniquely oriented, with its N-H bond directed toward the bilayer surface (Hu et al., 1993). Such orientation favors hydrogen bonding to the hydrophilic interface, presumably to water molecules that either are at the membrane surface or penetrate into the amphiphilic domain along the lipid-peptide interface. Second, the side chains of the tryptophan residues are extended parallel to the bilayer surface and are likely to be hydrogen-bonded to the lipid molecules (Meulendijks et al., 1989; Scarlata, 1991). These extended tryptophan side chains anchor the channel in the bilayer and orient the channel with respect to the surface. The tryptophan hydrogen bonding and indole electric dipole moments have been shown (Hu and Cross, 1995) to stabilize cations in the binding sites near the channel entrance and substantially reduce the potential energy barrier at the bilayer center. It has also been shown that the dynamics of the indole rings cause significant fluctuations in the energy of stabilization at the binding site, resulting in a possible mechanism for the rapid control of

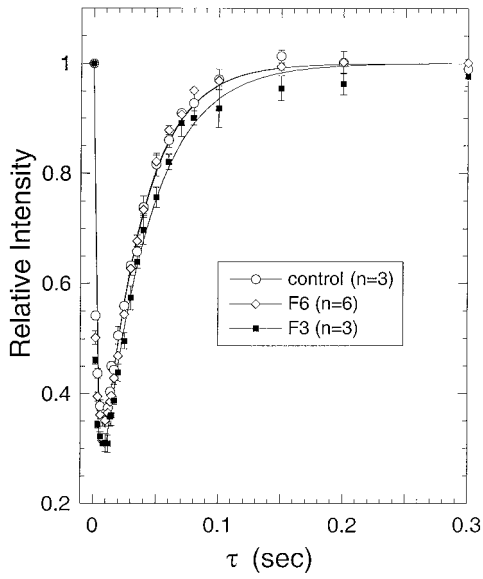

FIGURE 5 The signal intensity profiles of $^{23}Na^+_{in}$ are plotted as a function of $^{23}Na^+_{out}$ inversion recovery time, τ. Solid lines are best fit to the data using Eq. 4. At 75 μM gramicidin A in 66 mM PC/PG large unilamellar vesicles, 6.9 mM F3 increased the ^{23}Na apparent influx rate constant, k_i, from 182.1 ± 15.4 of control to 222.8 ± 21.7 s^{-1} ($n = 3$, $p < 0.05$), and the apparent efflux rate constant, k_e, from 149.7 ± 7.2 to 191.7 ± 12.2 s^{-1} ($n = 3$, $p < 0.001$). A similar concentration of F6 (6.3 mM) did not significantly affect the sodium transport, with $k_i = 176.9 \pm 17.8$ s^{-1} ($n = 6$, $p > 0.5$) and $k_e = 162.2 \pm 8.9$ s^{-1} ($n = 6$, $p > 0.2$). Error bars show the standard error of the mean.

the channel conductance (Hu and Cross, 1995). Thus, based on our TNOE results (Fig. 3), it is conceivable that because of their amphipathic properties and their preferential distribution to the interfacial region, anesthetics, but not nonimmobilizers, can target the tryptophan side chains and alter their functional association with the peptide-lipid-water interface.

Our MIT experiments of sodium transport across gramicidin channel provide direct evidence in support of this argument. The transport rates determined by the MIT method are consistent with the simple diffusion model described by the Goldman-Hodgkin-Katz equation. For 10 mM intra- and extravesicular [K^+], 100 mM intravesicular [Na^+], and 127 mM extravesicular [Na^+] (because of the shift reagent), the zero-current potential can be estimated to be 4.7 mV, provided that the permeability ratio of K^+ to Na^+ in gramicidin A channels is ~3.5 (Myers and Haydon, 1972; Urban et al., 1980). At this potential, Ussing's flux-ratio criterion (Ussing, 1949) predicts that the k_i-to-k_e ratio should be 1.2. Our results under the control condition are in excellent agreement with this prediction (Fig. 5, $k_i/k_e \approx 182/150 = 1.21$).

The rate constants k_i and k_e measured in the MIT experiments can also be used to estimate the absolute reaction rate constant for a single-ion transport across a single gramicidin A channel. Goulian et al. (1998) measured the dimer lifetime (τ) of gramicidin A and [Gly^1]gramicidin A, as well as the dimer formation rate (f) of [Gly^1]gramicidin A. Although the lifetimes of gramicidin and [Gly^1]gramicidin are different, the formation rate constant of the two should be similar (Dimer formation rate constant $= f/N_m^2$, where N_m is the number of monomers). Using a lipid surface density of 0.7 nm^2 per lipid dimer (Huang et al., 1994) and the gramicidin-to-lipid ratio used by Goulian et al. (1998), we estimated a dimer formation rate constant of 3×10^{-4} mol^{-1} s^{-1}, based on the measured formation rate of $f \approx 0.4$ mol/s. At steady state, $f\tau$ equals the number of gramicidin dimers (Goulian et al., 1998). Therefore, for $\tau \approx 8$–10 s (Goulian et al., 1998), ~20–25% of gramicidin molecules (i.e., ~16 μM monomers in our case) form ion-conducting channels at any given time (i.e., ~8 μM functional channel dimers). Thus, for a rate constant of ~200 s^{-1} measured by our MIT experiments, the absolute reaction rate constant through a single channel can be estimated to be $k_i^{abs} = k_i[Na^+]_e/[\text{channel}] = 3.2 \times 10^6$ s^{-1}. According to the absolute reaction rate theory, $k_i^{abs} = \kappa(kT/h)\exp(-\Delta G^{\neq}/RT)$, where $\Delta G^{\neq}$ is the free energy of activation associated with the transport, and κ is the probability that a sodium ion will advance through the channel, rather than exiting from the same side of the channel, after reaching the top of the $\Delta G^{\neq}$ barrier. Because the gramicidin A channel acts as a symmetrical electrical image barrier (Hinton et al., 1994), it follows that $\kappa \approx 0.5$. Thus the rate constants measured by the MIT experiments correspond to a $\Delta G^{\neq}$ of ~34 kJ/mol, which is within the range reported in the literature (Hinton et al., 1994).

Microscopically, sodium transport is believed to involve five distinct steps (Andersen, 1983; Buster et al., 1988): 1) diffusion through the aqueous phase to the channel entrance, 2) association with the channel entrance (binding), 3) translocation through the channel (in a single file), 4) dissociation from the channel, and 5) diffusion away from the channel. Patch-clamp measurements, with sensitivity high enough to monitor single-channel events, suggest that the transport is diffusion-limited (Andersen, 1983), with the aqueous convergence conductance being the most significant factor in determining the permeability characteristics of the gramicidin A channel. Thus one possible interpretation of the anesthetic and nonimmobilizer effects on transport is that anesthetics, but not nonimmobilizers, can facilitate tryptophan (particularly indole ring) interaction with the interfacial water to stabilize the sodium binding at the channel entrance, thereby increasing the unidirectional transport rates (Fig. 5). A similar increase in ion transport was also found for a wide range of general anesthetics, including halothane, enflurane, methoxyflurane, and ethanol (Hunt and Veiro, 1986).

Infrared spectroscopic studies (Buchet et al., 1985) have shown that volatile anesthetics can disrupt the hydrogen bonds at the center of the lipid membrane, where the carbonyls are involved in the head-to-head dimerization of the gramicidin channel. These results have been taken to support an earlier finding (Bradley et al., 1981) that anesthetics at physiological concentrations can reduce the lifetime of

N-acetyl-gramicidin dimers by a factor of 2 without affecting the single-channel current. This reduction was interpreted as anesthetic suppression of ion transport across the gramicidin channel, an apparent contradiction of the transport results found in this study with F3 and in other studies with a number of volatile anesthetics (Hunt and Veiro, 1986). The discrepancy may result from the difference between gramicidin and *N*-acetyl-gramicidin; the latter is known to form unstable channels (Urry, 1971). However, it has been shown (Finkelstein and Andersen, 1981) that a gramicidin channel is capable of transporting 2.6×10^6 ions/s, with a time constant of 0.38 μs for a single file of ions. In contrast, the lifetime of gramicidin dimers is $\sim$10 s (Goulian et al., 1998). Thus, on the time scale of ion translocation (step 3), the gramicidin channel can be viewed as a stable (or fixed) structure (Andersen, 1983). Therefore, a reduction by a factor of 2 in channel lifetime by anesthetics (Bradley et al., 1981) is unlikely to be the mechanism for anesthetic effects on channel conductance.

In conclusion, a pair of structurally similar anesthetic and nonimmobilizer interacts differently with a transmembrane channel peptide. Only the anesthetic, but not the nonimmobilizer, can interact specifically with the amphipathic domains near the channel-lipid-water interface. This interaction has direct functional consequences.

The authors thank Dr. Dexi Liu for help with LUV preparation and Dr. Leonard Firestone for encouragement and support.

This work was supported by grants from the National Institute of General Medical Sciences GM56257 (PT) and GM49202 (YX), and from the University Anesthesiology and Critical Care Medicine Foundation, University of Pittsburgh.

REFERENCES

Andersen, O. S. 1983. Ion movement through gramicidin A channels. Single-channel measurements at very high potentials. *Biophys. J.* 41: 119–133.

Arseniev, A. S., I. L. Barsukov, V. F. Bystrov, A. L. Lomize, and A. Ovchinnikov Yu. 1985. ^{1}H-NMR study of gramicidin A transmembrane ion channel. Head-to-head right-handed, single-stranded helices. *FEBS Lett.* 186:168–174.

Bradley, R. J., D. W. Urry, G. Parenti-Castelli, and G. Lenaz. 1981. Effects of halothane on channel activity of N-acetyl gramicidin. *Biochem. Biophys. Res. Commun.* 101:963–969.

Buchet, R., C. Sandorfy, T. L. Trapane, and D. W. Urry. 1985. Infrared spectroscopic studies on gramicidin ion-channels: relation to the mechanisms of anesthesia. *Biochim. Biophys. Acta.* 821:8–16.

Buster, D. C., J. F. Hinton, F. S. Millett, and D. C. Shungu. 1988. ^{23}Na-nuclear magnetic resonance investigation of gramicidin-induced ion transport through membranes under equilibrium conditions. *Biophys. J.* 53:145–152.

Cafiso, D. S. 1998. Dipole potentials and spontaneous curvature: membrane properties that could mediate anesthesia. *Toxicol. Lett.* 100–101: 431–439.

Chu, S. C., M. M. Pike, E. T. Fossel, T. W. Smith, J. A. Balschi, and C. S. Springer. 1984. Aqueous shift reagents for high-resolution cationic nuclear magnetic resonance. III. $Dy(TTHA)^{3-}$, $Tm(TTHA)^{3-}$, and $Tm(PPP)_2^{3-}$. *J. Magn. Res.* 56:33–47.

Cross, T. A. 1994. Structural biology of peptides and proteins in synthetic membrane environments by soild-state NMR spectroscopy. *Annu. Rep. NMR Spectrosc.* 29:123–167.

Cross, T. A. 1997. Solid-state nuclear magnetic resonance characterization of gramicidin channel structure. *Methods Enzymol.* 289:672–696.

Cubero, E., F. J. Luque, and M. Orozco. 1998. Is polarization important in cation-pi interactions? *Proc. Natl. Acad. Sci. USA.* 95:5976–5980.

Eckenhoff, R. G., and J. S. Johansson. 1997. Molecular interactions between inhaled anesthetics and proteins. *Pharmacol. Rev.* 49:343–367.

Finkelstein, A., and O. S. Andersen. 1981. The gramicidin A channel: a review of its permeability characteristics with special reference to the single-file aspect of transport. *J. Membr. Biol.* 59:155–171.

Forman, S. A., and D. E. Raines. 1998. Nonanesthetic volatile drugs obey the Meyer-Overton correlation in two molecular protein site models. *Anesthesiology.* 88:1535–1548.

Franks, N. P., and W. R. Lieb. 1994. Molecular and cellular mechanisms of general anaesthesia. *Nature.* 367:607–614.

Franks, N. P., and W. R. Lieb. 1996. An anesthetic-sensitive superfamily of neurotransmitter-gated ion channels. *J. Clin. Anesth.* 8:3S–7S.

Glantz, S. A., and B. K. Slinker. 1990. Primer of Applied Regression and Analysis of Variance. McGraw-Hill Health Professions Division, New York.

Goulian, M., O. N. Mesquita, D. K. Fygenson, C. Nielsen, O. S. Andersen, and A. Libchaber. 1998. Gramicidin channel kinetics under tension. *Biophys. J.* 74:328–337.

Gupta, R. K., and P. Gupta. 1982. Direct observation of resolved resonances from intra- and extracellular sodium-23 ions in NMR studies of intact cells and tissues using dysprosium(III)tripolyphosphate as paramagnetic shift reagent. *J. Magn. Reson.* 47:344–350.

Hinton, J. F. 1996. Cation-binding location and hydrogen-exchange sites for gramicidin in SDS micelles using NOESY NMR. *J. Magn. Reson. B.* 112:26–31.

Hinton, J. F., D. K. Newkirk, T. G. Fletcher, and D. C. Shungu. 1994. Application of the magnetization-inversion-transfer technique to the transport of $^7Li^+$, $^{23}Na^+$, and $^{39}K^+$ ions through the gramicidin channel and the M2 delta transmembrane domain of the nicotinic acetylcholine receptor. *J. Magn. Reson B.* 105:11–16.

Hu, W., and T. A. Cross. 1995. Tryptophan hydrogen bonding and electric dipole moments: functional roles in the gramicidin channel and implications for membrane proteins. *Biochemistry.* 34:14147–14155.

Hu, W., K. C. Lee, and T. A. Cross. 1993. Tryptophans in membrane proteins: indole ring orientations and functional implications in the gramicidin channel. *Biochemistry.* 32:7035–7047.

Huang, P., J. J. Perez, and G. H. Loew. 1994. Molecular dynamics simulations of phospholipid bilayers. *J. Biomol. Struct. Dyn.* 11: 927–956.

Hunt, G. R. A., and J. A. Veiro. 1986. The use of ^{23}Na and ^{7}Li nuclear magnetic resonance spectroscopy to study alkali metal ion transport across gramicidin channels in large unilamellar phospholipid vesicles, and the effect of general anesthetics. *Biochem. Soc. Trans.* 14:602–603.

Ionescu, P., E. I. Eger, and J. Trudell. 1994. Direct determination of oil/saline partition coefficients. *Anesth. Analg.* 79:1056–1058.

Kendig, J. J., A. Kodde, L. M. Gibbs, P. Ionescu, and E. I. Eger. 1994. Correlates of anesthetic properties in isolated spinal cord: cyclobutanes. *Eur. J. Pharmacol.* 264:427–436.

Ketchem, R., B. Roux, and T. Cross. 1997. High-resolution polypeptide structure in a lamellar phase lipid environment from solid state NMR derived orientational constraints. *Structure.* 5:1655–1669.

Killian, J. A., T. P. Trouard, D. V. Greathouse, V. Chupin, and G. Lindblom. 1994. A general method for the preparation of mixed micelles of hydrophobic peptides and sodium dodecyl sulphate. *FEBS Lett.* 348:161–165.

Koblin, D. D., B. S. Chortkoff, M. J. Laster, E. I. Eger, M. J. Halsey, and P. Ionescu. 1994. Polyhalogenated and perfluorinated compounds that disobey the Meyer-Overton hypothesis. *Anesth. Analg.* 79:1043–1048.

Le Guerneve, C., and M. Seigneuret. 1996. High-resolution mono- and multidimensional magic angle spinning ^{1}H nuclear magnetic resonance of membrane peptides in nondeuterated lipid membranes and H_2O. *Biophys. J.* 71:2633–2644.

Mayer, L. D., M. J. Hope, and P. R. Cullis. 1986. Vesicles of variable sizes produced by a rapid extrusion procedure. *Biochim. Biophys. Acta.* 858: 161–168.

Meulendijks, G. H., T. Sonderkamp, J. E. Dubois, R. J. Nielen, J. A. Kremers, and H. M. Buck. 1989. The different influences of ether and ester phospholipids on the conformation of gramicidin A. A molecular modelling study. *Biochim. Biophys. Acta.* 979:321–330.

Mihic, S. J., Q. Ye, M. J. Wick, V. V. Koltchine, M. D. Krasowski, S. E. Finn, M. P. Mascia, C. F. Valenzuela, K. K. Hanson, E. P. Greenblatt, R. A. Harris, and N. L. Harrison. 1997. Sites of alcohol and volatile anaesthetic action on GABA(A) and glycine receptors. *Nature.* 389: 385–389.

Mobashery, N., C. Nielsen, and O. S. Andersen. 1997. The conformational preference of gramicidin channels is a function of lipid bilayer thickness. *FEBS Lett.* 412:15–20.

Myers, V. B., and D. A. Haydon. 1972. Ion transfer across lipid membranes in the presence of gramicidin A. II. The ion selectivity. *Biochim. Biophys. Acta.* 274:313–322.

Navon, G., Y.-Q. Song, T. Room, S. Appelt, R. E. Taylor, and A. Pines. 1996. Enhancement of solution NMR and MRI with laser-polarized xenon. *Science.* 271:1848–1851.

Noggle, J. H., and R. E. Schirmer. 1971. The Nuclear Overhauser Effect: Chemical Applications. Academic Press, New York.

North, C., and D. S. Cafiso. 1997. Contrasting membrane localization and behavior of halogenated cyclobutanes that follow or violate the Meyer-Overton hypothesis of general anesthetic potency. *Biophys. J.* 72: 1754–1761.

Raines, D. E. 1996. Anesthetic and nonanesthetic halogenated volatile compounds have dissimilar activities on nicotinic acetylcholine receptor desensitization kinetics. *Anesthesiology.* 84:663–671.

Scarlata, S. F. 1991. Effect of increased chain packing on gramicidin-lipid interactions. *Biochemistry.* 30:9853–9859.

Silver, M. S., R. I. Joseph, C. N. Chen, V. J. Sank, and D. I. Hoult. 1984. Selective population inversion in NMR. *Nature.* 310:681–683.

Tang, P., V. Simplaceanu, and Y. Xu. 1999. Structural consequences of anesthetic and nonimmobilizer interaction with gramicidin A channels. *Biophys. J.* 76:2346–2350.

Tang, P., B. Yan, and Y. Xu. 1997. Different distribution of fluorinated anesthetics and nonanesthetics in model membrane: a ^{19}F NMR study. *Biophys. J.* 72:1676–1682.

Trudell, J. R., D. D. Koblin, and E. I. Eger. 1998. A molecular description of how noble gases and nitrogen bind to a model site of anesthetic action. *Anesth. Analg.* 87:411–418.

Urban, B. W., S. B. Hladky, and D. A. Haydon. 1980. Ion movements in gramicidin pores. An example of single-file transport. *Biochim. Biophys. Acta.* 602:331–354.

Urry, D. W. 1971. The gramicidin A transmembrane channel: a proposed pi(L, D) helix. *Proc. Natl. Acad. Sci. USA.* 68:672–676.

Ussing, H. H. 1949. The distinction by means of tracers between active transport and diffusion. The transfer of iodide across the isolated frog skin. *Acta Physiol. Scand.* 19:43–56.

Weinstein, S., B. A. Wallace, E. R. Blout, J. S. Morrow, and W. Veatch. 1979. Conformation of gramicidin A channel in phospholipid vesicles: a ^{13}C and ^{19}F nuclear magnetic resonance study. *Proc. Natl. Acad. Sci. USA.* 76:4230–4234.

Xu, Y., and P. Tang. 1997. Amphiphilic sites for general anesthetic action? Evidence from ^{129}Xe-[^{1}H] intermolecular nuclear Overhauser effects. *Biochim. Biophys. Acta.* 1323:154–162.

Xu, Y., P. Tang, and S. Liachenko. 1998. Unifying characteristics of sites of anesthetic action revealed by combined use of anesthetics and non-anesthetics. *Toxicol. Lett.* 100:347–352.

Yoshino, A., T. Yoshida, H. Okabayashi, H. Kamaya, and I. Ueda. 1998. F-19 and H-1 NMR and NOE study on halothane-micelle interaction—residence location of anesthetic molecules. *J. Colloid Interface Sci.* 198:319–322.